X-ray absorption spectroscopy study of the chemical ordering in $UCu_{5-x}M_x$ (M = Ni, Ag) compounds

2008 J. Phys.: Condens. Matter 20 395207

(http://iopscience.iop.org/0953-8984/20/39/395207)

J. Phys.: Condens. Matter **20** (2008) 395207 (7pp) doi:10.1088/0953-8984/20/39/395207

X-ray absorption spectroscopy study of the chemical ordering in $UCu_{5-x}M_x$ (M = Ni, Ag) compounds

J Chaboy[1], R Boada[1], O J Durá[2] and M A López de la Torre[2]

[1] Instituto de Ciencia de Materiales de Aragón and Departamento de Física de la Materia Condensada, CSIC-Universidad de Zaragoza, 50009 Zaragoza, Spain
[2] Departamento de Física Aplicada and Instituto de Investigaciones Energéticas y Aplicaciones Industriales, Escuela Técnica Superior de Ingenieros Industriales, Universidad de Castilla-la Mancha, 13071 Ciudad Real, Spain

Received 2 June 2008, in final form 21 July 2008
Published 1 September 2008
Online at stacks.iop.org/JPhysCM/20/395207

Abstract

This work reports the x-ray absorption spectroscopy study of the chemical ordering in $UCu_{5-x}M_x$ (M = Ni, Ag) compounds. The comparison between the experimental Cu K-edge XANES spectra and theoretical computations based on multiple-scattering theory shows that standard single-channel calculations are capable of reproducing the experimental spectra. On this subject, an extensive discussion is presented concerning the role of both the cluster size and the final state potential in obtaining a good reproduction of the experimental XANES spectra of these UCu_5-based alloys. The agreement between the theoretical and experimental spectra points to the existence of crystallographic disorder in both UCu_4Ag and UCu_4Ni systems. Possessing the distinct low temperature electrical, magnetic and thermal properties exhibited by UCu_4Ni, our results suggest that Ni doping must induce dramatic changes in the electronic structure, as confirmed by the thermopower measurements. These results point to the imbalance between the RKKY and Kondo interactions as the source of the NFL behaviour observed in UCu_4Ni, thus supporting an interpretation of the NFL behaviour in terms of the Griffiths phase model.

(Some figures in this article are in colour only in the electronic version)

1. Introduction

Non-Fermi-liquid (NFL) behaviour in metals has received great attention in recent years from both experimental and theoretical points of view [1–4]. In these systems, the low temperature properties such as the electronic specific heat, magnetic susceptibility and electrical resistivity, are characterized by logarithmic or power-law temperature dependences that are in contrast to those of Fermi liquids. NFL behaviour of many of these Ce-, Yb-, or U-based heavy fermion materials is often observed when long-range magnetic order is suppressed by the substitution of a nonmagnetic element or by the application of pressure [1, 4]. More recently, special interest has been focused on the role that disorder can play in NFL behaviour, as many materials that exhibit NFL phenomena are intrinsically disordered alloys. In this way, different models based in disorder-driven mechanisms have been proposed to account for non-Fermi-liquid behaviour. The *Kondo disorder* model (KDM) [5] is essentially a single-impurity model with a distribution of Kondo temperatures, and might be considered as a disordered Fermi-liquid model. The KDM utilizes a distribution of Kondo temperatures caused by a distribution of f-electron/conduction electron exchange coupling strengths, possibly induced by lattice disorder. Castro Neto *et al* [6] proposed a model which describes the competition the RKKY and Kondo interactions in a disordered material leading to the formation of magnetic clusters and Griffiths-McCoy singularities. Recently, Miranda and Dobrosavljevic investigated a disordered Anderson lattice and proposed that a Griffiths phase could be obtained by a disorder-driven metal–insulator transition [7].

Consequently, determining the nature of the lattice disorder in NFL systems represents a key issue in the understanding of the underlying mechanism for NFL behaviour. Aiming at this, we have carried out an x-ray absorption spectroscopy (XAS) investigation on the $UCu_{5-x}M_x$ system, whose electrical, magnetic and thermal properties have been reported to show NFL behaviour in

the case of M = Pd, Ni [8, 9]. As the main objective of this work is to determine the crystallographic disorder in the $UCu_{5-x}M_x$ system, the use of XAS is highly appropriate as nowadays it constitutes an outstanding structural tool. In this way, the extended x-ray absorption fine structure (EXAFS) part of the spectrum is commonly used to determine the local environment around a selected atomic species in a great variety of systems [10]. Moreover, the near-edge part of the absorption spectrum (XANES) becomes an incomparable stereochemical probe because of its high sensitivity to the bonding geometry. This capability is due to the low kinetic energy of the photoelectron thus favouring the contribution of multiple-scattering processes. For this reason, a great effort has been devoted in the last decade to obtain structural determinations from XANES, including bond-angle information. However, the interpretation and the *ab initio* computation of XANES spectra are not as straightforward as for EXAFS. The computation of XANES needs sophisticated computing codes, mostly based on the one-electron multiple-scattering (MS) theory [11]. Typically, these *ab initio* codes use the muffin-tin approximation [12, 13], although recent works have shown the promising capabilities of non-muffin-tin approaches [14–16]. Nowadays, the construction of the scattering potential and the treatment of the inelastic losses of the photoelectron still remain as open problems in XANES computations. The accumulated experience through the calculation of the absorption cross section for different systems indicates that the choice of the exchange–correlation potential (ECP) is one the most important steps in obtaining a good reproduction of the experimental spectra [17–19]. Consequently, special attention has to be paid to determining the adequate ECP needed for the calculations.

In this work we have taken advantage of the XANES capabilities to study the substitution of both Ag and Ni within the UCu_5 frame. In particular the stereochemical sensitivity of XANES provides a direct tool to determine which crystallographic site is occupied by the substituted metals (Ag and Ni) in several UCu_4M compounds. To this end, we have performed detailed *ab initio* multiple-scattering computations for the Cu K-edge XANES spectra in these compounds. The comparison of the experimental and theoretical spectra indicates the existence of Ag/Cu and Ni/Cu site interchange in UCu_4Ag and UCu_4Ni compounds, respectively. The XANES results show the existence of crystallographic disorder in both systems, excluding structural effects, through the preferential substitution of Ag and Ni at the 4c positions, at the origin of the observed NFL behaviour. On the contrary they point to the modification of the electronic structure of UCu_5 induced by the Ni and Ag doping. This has been demonstrated by the results of thermopower measurements. These results have been discussed in terms of the relationship between the imbalance of the RKKY and Kondo interactions and the NFL behaviour observed in UCu_4Ni.

2. Experimental and computational methods

Cu K-edge XAS spectra were recorded for UCu_5, UCu_4Ni and UCu_4Ag at the BM25A SPline beamline of the ESRF. Details of sample preparation and characterization can be found elsewhere [20, 21]. The storage ring was operated in the 16 bunch mode with a typical current of ∼90 mA at an electron beam energy of 6 GeV. Measurements were performed at room temperature in the fluorescence detection mode on bulk UCu_5, UCu_4Ag and UCu_4Ni samples. The fixed-exit double-crystal monochromator was equipped with a pair of Si(111) crystals giving the energy resolution $\Delta E/E \sim 7 \times 10^{-5}$ at the Cu K-edge (8979 eV). Harmonic rejection was achieved by detuning the second crystal from parallel alignment to 50% intensity. Fluorescence spectra were recorded with the sample aligned at 45° with respect to the incident beam, using a single-element Ge solid state detector. In all cases the onset energy of the absorption process was chosen to be the maximum of the first derivative in the edge region of the absorption spectrum. The experimental XANES spectra were normalized at high energy, after background subtraction, to eliminate thickness dependence.

The computations of the XANES spectra were carried out using the multiple-scattering code CONTINUUM [12] based on the one-electron full-multiple-scattering theory [11, 22]. A complete discussion of the procedure can be found in [23, 24]. The potential for the different atomic clusters was approximated by a set of spherically averaged muffin-tin (MT) potentials built following the standard Mattheis prescription [25]. The muffin-tin radii were determined following Norman's criterion [26]. The Coulomb part of each atomic potential was generated using charge densities from the atomic code of non-local self-consistent Dirac–Fock code [13, 27]. We have also verified that using charge densities for neutral atoms obtained from the tabulated atomic wave functions by Clementi and Roetti [28] does not modify the results. Atomic orbitals were chosen to be neutral for the ground state potential and different approximations were tested for the excited state potential. During the present calculations we have found that the screened and relaxed $Z + 1$ option [29] leads to the best performance in simulating the experimental absorption spectra at the Cu K-edge [29]. In all cases, the calculated theoretical spectra have been further convolved with a Lorentzian shape function $\Gamma = 1.5$ eV to account for both the core–hole lifetime [30] and the experimental resolution.

Thermopower measurements were performed using a commercial MMR technologies system. The Seebeck coefficient $S(T)$ is obtained by comparison with a reference constant wire. The three samples studied in this work had similar dimensions (∼1 mm × 1 mm × 6–8 mm). To check the reproducibility of these measurements we repeated the experimental runs with new contacts both on the sample and on the reference constant wire. From our results, we estimate that the experimental accuracy of the measurements shown in this work is better than ±5%.

3. Results and discussion

The UCu_5 and the substituted UCu_4Ag and UCu_4Ni compounds show the face-centred cubic structure $AuBe_5$-type (space group $F43m$). The lattice parameters are $a = 7.033$ Å for UCu_5 [35]; $a = 7.11$ Å for UCu_4Ag [31]; and $a = 6.983$ Å

for UCu_4Ni [36]. In the UCu_5 compound the Cu atoms occupy 4c (1/4, 1/4, 1/4) and 16e (0.625, 0.625, 0.625) positions, and U atoms are at the 4a (0, 0, 0) positions.

In the case of UCu_4Ag it has been reported that it is not possible to state definitely from x-ray diffraction measurements alone whether the Ag atoms are randomly distributed in the two sites (4c and 16e) of the unit cell or they exhibit a certain preference of occupation [31]. Based on NMR measurements, Umari *et al* conclude that Ag has a strong preference to occupy the (4c) sites [31]. These authors discuss the existence of site interchange on the basis of atom sizes. Accordingly, as the radius of Ni atom is smaller than that of Cu, the Ni atoms should be randomly distributed over the (16e) sites. Extending the same reasoning to those atoms being bigger than Cu, it is concluded that Ag and Pd occupy only the (4c) sites in UCu_4Ag and UCu_4Pd, respectively.

However, the results reported in the case of UCu_4Pd exemplify both, the limitation of this steric model as well as how the existing controversy regarding the chemical ordering in $UCu_{5-x}M_x$ compounds prevents the exact understanding of their magnetic behaviour. A claim for crystallographic evidence of chemical ordering in the $UCu_{5-x}Pd_x$ system was reported by Chau *et al* based on neutron diffraction measurements [32]. According to these authors both the Pd and Cu atoms occupy separate crystallographic sites in UCu_4Pd, as the accuracy of their analysis is good enough to exclude the complete Pd/Cu randomness that would imply 20% occupancy of (16e) sites. Moreover, they assert that their results are in agreement with the earlier NMR studies by Bernal *et al* [5]. Surprisingly, Bernal *et al* held the contrary opinion pointing out that despite XRD suggesting that UCu_4Pd is an ordered compound [8], this cannot entirely be the case, since the NMR broadening is an unambiguous indicator of magnetic disorder. More recently, Booth *et al* [33] addressed that their previous analysis [32] cannot differentiate between full 4c site occupancy by Pd and up to approximately 16% of the 4c sites being occupied by Cu rather than Pd atoms. The same work reports an EXAFS study performed at the U L_3-edge, and at the K-edge of both Cu and Pd. While inconclusive results are inferred from the analysis of the U and Cu EXAFS, the existence of Pd/Cu interchange is concluded from the analysis of the Pd K-edge (a $\sim$1/4 fraction of the Pd atoms occupy the nominally Cu 16e sites). A more sophisticated EXAFS analysis reported by the same group also addressed the existence of site interchange [34]. However, the EXAFS analysis of the Pd, U, and Cu absorption spectra does not yield a unique answer showing, on the contrary, differences regarding not only the fraction of Pd atoms on the 16e sites, but also in the Pd–Cu interatomic distances or Debye–Waller factors.

These results point out that EXAFS analysis is not conclusive in deciding if the system is intrinsically homogeneous or not. By contrast, the study of the XANES part of the spectrum, showing a higher sensitivity to the bonding geometry, might offer a clarification of the current controversy existing regarding the M/Cu site interchange in UCu_4M compounds. Therefore, we have compared the experimental Cu K-edge XANES spectra to theoretical *ab initio* XANES calculations performed at the Cu K-edge in the case of UCu_5 and of the substituted UCu_4Ag and UCu_4Ni samples.

The first step of the calculations was to determine the size of the cluster needed to reproduce all the spectral features present in the experimental XANES spectra. To this end we performed the computation of the Cu K-edge XANES in the case of UCu_5 progressively increasing the number of atoms in the cluster. It should be noted that because Cu occupies two different, 4c and 16e, crystallographic positions XANES computations have to be performed for two different clusters in which the absorbing Cu atom lies at the 4c (Cu1) and at the 16e (Cu2) positions, respectively. Then, the theoretical spectra are made up from the weighted sum of both contributions according the crystallographic statistical ratio, i.e. Cu1 and Cu2 spectra contribute 20% and 80% to the total UCu_5 spectrum, respectively. In this way we have determined that the computations performed for a cluster including contributions from neighbouring atoms located within the first 6 Å around photoabsorbing Cu account for all the observed spectral features. Such a cluster contains 69 atoms in the case of absorption at the Cu1 sites and 63 in the case of Cu2. The addition of further coordination shells does not contribute significantly to the XANES spectrum. It should be noted that the assessment of the quality of the theoretical computations is based on the correct reproduction of the shape and energy position of the different spectral features and of their relative energy separation and intensity ratio as well. Accordingly, all the calculations reported henceforth have been obtained by using clusters containing 69 and 63 atoms to generate both the scattering potential and the scattering contributions at both Cu1 and Cu2 sites, respectively. We have also determined the maximum angular momentum quantum number, l_{max}, needed to account for the experimental spectrum in the first 70 eV of the absorption spectrum, i.e. where the main spectral features appear. The choice of $l_{max} = 3$ and 4 does not affect the result of the computations in this region and, consequently, we have fixed $l_{max} = 3$ for all the calculations. We have also studied the effect of the overlapping factor imposed on the muffin-tin spheres to build up the potential [26] in reproducing the Cu K-edge XANES spectrum. We have verified that this factor affects both the shape and the intensity of the computed spectral features. The best reproduction of the experimental UCu_5 spectrum is obtained by using a 10% overlapping factor to build up a 6 Å cluster.

Once we have fixed both the cluster size and l_{max}, we investigated the role of the different exchange and correlation potentials (ECP) in correctly reproducing the experimental spectra. We have computed the Cu K-edge XANES of UCu_5 by using the energy-dependent Dirac-Hara (DH) and Hedin-Lundqvist (HL) ECP potentials [18, 19]. The HL is a complex potential in which the imaginary accounts for the inelastic losses of the photoelectron. Hence, we have also performed the computations by using only the real part of the HL ECP (hereafter, real HL). Finally, we have built a 'complex' Dirac-Hara potential by adding the imaginary part of the HL ECP to the real DH ECP [18, 19]. As a general result we have found a good agreement between the experimental and theoretical spectra when computations are made by using real

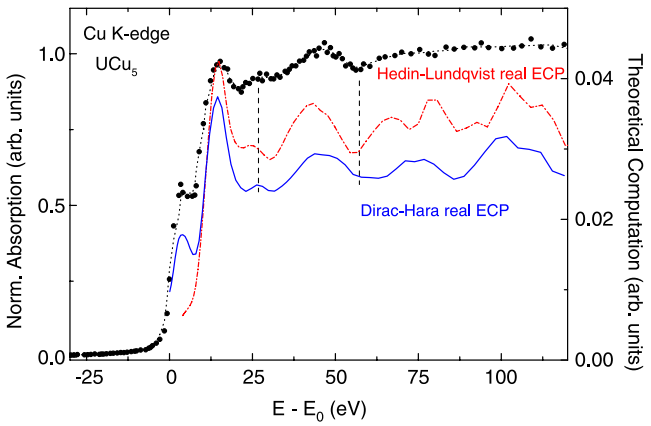

Figure 1. Comparison between the experimental (●) Cu K-edge of UCu_5 and the result of the MS computations performed for a cluster of 6 Å around the absorbing Cu and by using both real HL (red, dot–dash line) and DH (blue, solid line) ECP potentials.

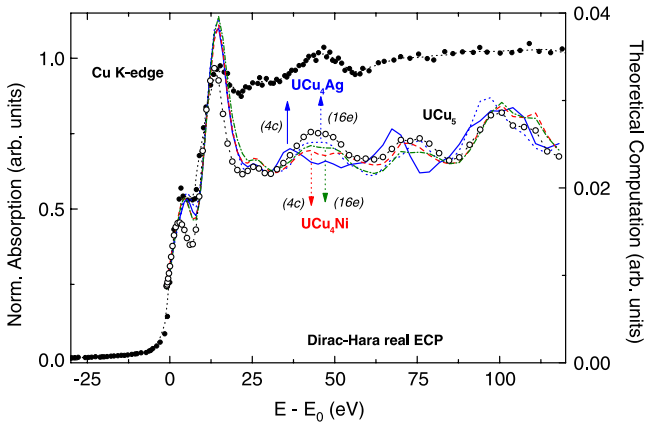

Figure 2. Comparison between the MS computations performed for a UCu_4Ag cluster by considering either that the Ag atoms occupy the 4c position exclusively (solid line, blue), or that they are distributed on the 16e sites (dots, blue). Similar computations for UCu_4Ni are reported: 4c sites (dash, red) and 16e (dot–dash, green). For the sake of completion the experimental Cu K-edge XANES spectrum of UCu_5 (●) and its computation (○, black) are also included.

ECP potentials. In contrast, the agreement worsens in the case of using complex potentials, as the imaginary part of the HL ECP introduces an excessive damping of the signal that leads to missing several absorption features. Figure 1 reports the comparison between the theoretical spectra computed by using both real HL and DH and the experimental spectrum of UCu_5. The computation performed by using the real Dirac-Hara exchange and correlation potential reproduces all the spectral features as well as their energy separation. In contrast, the agreement between experimental and computed spectra worsens in the case of the computations performed by using the real HL potential. In addition to the poor reproduction of the intensity of the spectral features the calculated absorption maxima fall short of the observed ones.

Following these prescriptions, we have extended our computations to the Cu K-edge XANES spectra of both UCu_4Ag and UCu_4Ni compounds. Because several reports suggested that chemical ordering may be involved in the substitution [5, 8, 31–34], we have tried to disentangle the effect of the structural modification, concerning the modification of the cell parameters and interatomic distances, and that of the different backscattering power of the substituent Ag and Ni atoms with respect to Cu. Aiming at this, we have computed the Cu K-edge XANES spectra for UCu_5 clusters in which the cell parameters correspond to those of UCu_4Ag and UCu_4Ni compounds without substituting Cu either by Ag or Ni. In this way we have verified that the expansion–contraction of the crystal cell has little influence into the overall spectral shape and only slight differences in the intensity of the computed spectral features are found within the energy range of our interest. Therefore, we have performed the computations for real UCu_4Ag and UCu_4Ni clusters, i.e. including Ag and Ni atoms as scatterers. These computations have been performed by considering that: (i) all the substituent (Ag or Ni) atoms enters the 4c position, and (ii) Ag and Ni enter only at the 16e sites. The results of these calculations are shown in figure 2. In the case of UCu_4Ni no significant difference is found for both occupation schemes. By contrast, they show significant differences in the case of UCu_4Ag. If all the Ag atoms occupy the 4c positions the computed spectral shape differs from that of UCu_5: a new spectral feature appears at ∼35 eV above the edge and, at the same time, the broad resonance centred at ∼42 almost disappears. As shown in figure 2 this result is not supported by the experimental observation. Therefore, we can rule out the preferential scheme or *chemical ordering* scheme previously suggested because, despite the 4c sites being larger and, more capable of accommodating the Ag atoms, the XANES results indicate that there is no fully preferential occupation of these sites by Ag. Finally, we report in figure 3 the result of the computations performed considering that the Ag atoms occupy both 4c and 16e sites according to statistical probability, and by considering a 50% preferential occupancy of the 4c sites. As shown in comparison, the best reproduction of the experimental spectrum is obtained when the Ag atoms are placed within the UCu_5 frame without any preferential occupation scheme.

The comparison of the experimental and theoretical spectra unambiguously indicates the existence of Ag/Cu and Ni/Cu site interchange in UCu_4Ag and UCu_4Ni compounds, respectively. These results indicate that the preferential substitution of Ag at the 4c positions, previously suggested [31], does not take place in UCu_4Ag. They offer not only a clarification regarding the M/Cu site interchange in UCu_4M compounds but also might lead to a deeper insight into the influence of the substituent on the magnetic properties of the system, especially regarding the applicability of Kondo disorder models of the NFL behaviour observed for M = Ni. Our results indicate that the appearance of NFL properties in UCu_4M does not essentially depend upon whether M atoms go to the 4c or 16e sites in the $AuBe_5$ structure. Indeed, according to the XANES results both UCu_4Ag and UCu_4Ni compounds exhibit site interchange and, thus, lattice disorder. However, while the Ni substitution has a destructive effect on the stability of long-range magnetic order, it is manifest that Ag has the

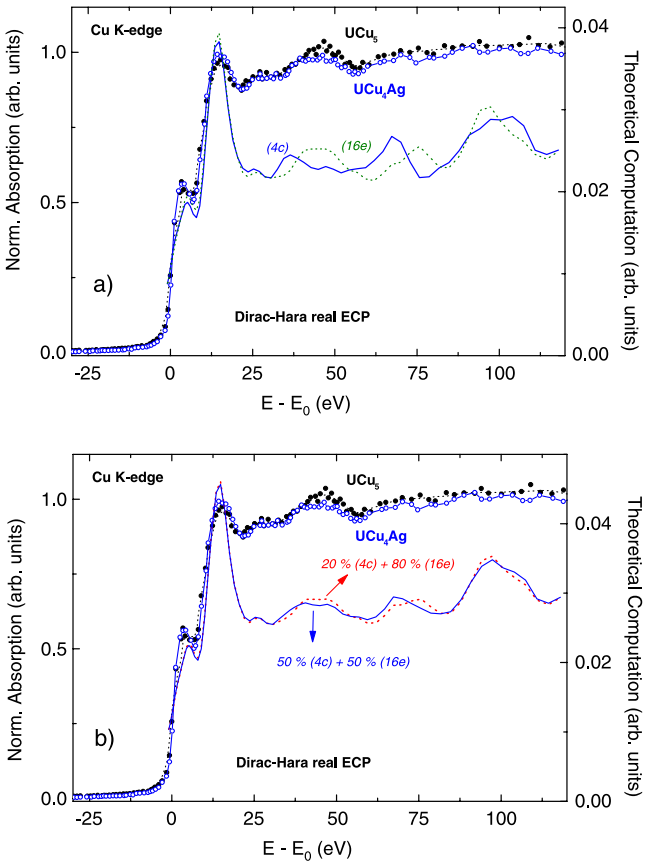

Figure 3. (a) Comparison of the Cu K-edge XANES spectra of UCu_5 (black, ●) and UCu_4Ag (blue, ○) and the computations performed for a 6 Å UCu_4Ag cluster by considering either that the Ag atoms occupy the 4c position (blue, solid line), or that they are distributed on the 16e sites (dot, green). In panel (b) a similar comparison is made by considering that the Ag atoms are statistically distributed on both 4c and 16e sites (dots, red), and that half of the Ag atoms occupy the 4c(16e) positions (solid line, blue).

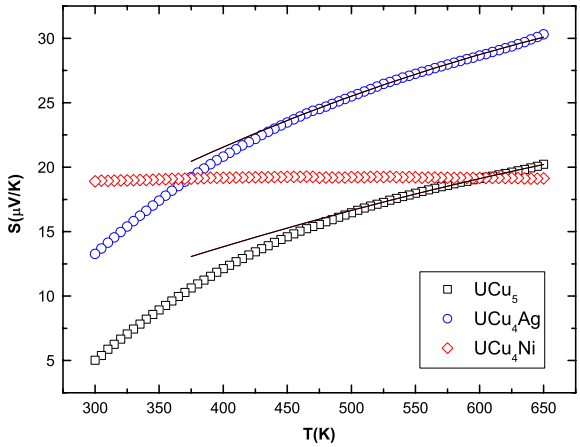

Figure 4. Seebeck coefficient of UCu_5, UCu_4Ag and UCu_4Ni. Room temperature results are in good agreement ($\pm 2\ \mu V\ K^{-1}$) with previous results by van Daal *et al* [40].

opposite effect [20, 21]. Therefore, these results suggest that the evolution of the magnetic properties with doping is mainly associated with the specific electronic characteristics of the substituent rather than with structural or lattice disorder effects.

Within the standard Kondo lattice theory framework [37] the progressive doping with Ni (and Pd) is expected to produce significant changes in the electronic structure of the $UCu_{5-x}M_x$ compounds. As a result there should be an imbalance between the RKKY and Kondo interactions since the relative strength of both interactions is extremely sensitive to changes in the density of states. This is in agreement with the fast reduction of the Nèel temperature observed both for Ni (Pd) doping, which approaches $T = 0$ for $x \sim 1$ [8, 9]. In the particular case of Ni doping, the progressive destruction of the long-range magnetic order is accompanied by a sizeable reduction of the electronic specific-heat coefficient, from $\gamma =$ 300 mJ mol^{-1} K^{-2} at $T = 2$ K observed in UCu_5 [38] to $\gamma =$ 100–110 mJ mol^{-1} K^{-2} [36, 39]. In contrast, doping with Ag, more similar to Cu, is not expected to generate such electronic effects resulting in a much weaker imbalance between the two competing interactions. As a matter of fact, instead of a destructive effect, even a moderate enhancement of T_N is observed for UCu_4Ag [20, 21]. Moreover, the low temperature transport, magnetic and thermal properties of this system are essentially similar to those of UCu_5, not showing any signature suggestive of NFL behaviour. To give a significant example, the electronic specific-heat coefficient remains practically unchanged in respect to UCu_5 [38]. As $\gamma \propto 1/T_K$, this implies an enhanced T_K with Ni doping, in agreement with the hypothesis of an imbalance between the RKKY and Kondo interactions proposed above.

In order to experimentally verify the different electronic effect of doping with Ag or Ni, we have performed a comparative study of thermopower $S(T)$ in UCu_5, UCu_4Ni and UCu_4Ag. Although $S(T)$ measurements are sensitive to changes of the density of states at the Fermi surface, in the case of heavy fermion systems they are difficult to interpret, especially at low temperatures, owing to the superposition of different scattering contributions due to electronic diffusion, magnetic order and/or Kondo effect, and phonon-drag. Therefore, we have focused on the high temperature regime of $S(T)$ ($T > 300$ K) in order to simplify the analysis. The results for UCu_5 and UCu_4Ni reported in figure 4 are in good agreement with previous results in the temperature range 10–300 K [40]. Notice the similarity between the curves obtained for UCu_5 and UCu_4Ag. They are nearly parallel between 300 and 650 K, both approaching a linear temperature dependence in the high temperature limit. Following the classical Mott theory of thermopower in metals [41], this would suggest that $S(T)$ of both systems is dominated, at high temperatures, by an electron diffusion term. Moreover, the similar positive slope of both curves implies a similar electronic structure, since this slope is proportional to the logarithmic derivative of the density of states at the Fermi energy E_F, and inversely proportional to E_F [41, 42]:

$$S_d = \frac{\pi^2 k_B^2}{3e} T \left(\frac{\partial \ln n(E)}{\partial E} \right)_{E_F} = \frac{\pi^2 k_B^2}{3e E_F} T \left(\frac{\partial \ln n(E)}{\partial \ln E} \right)_{E_F}. \quad (1)$$

Although the simple analysis above is useful to illustrate the comparable electronic properties of these two systems, its

application to these strongly correlated electron systems might be criticized. For that reason, we have attempted a more elaborated approach, following a modified version of Mott's formula [43], based on the phenomenological Hirst resonance model [44], which is often used to analyse the high temperature thermopower of heavy fermion systems [45]. This model assumes that $S(T)$ is dominated by a contribution caused by scattering between electrons at a broad s-band and others at a narrow f-band with a Lorentzian shape. At high temperature, where the phonon, magnetic and/or Kondo contributions are negligible, the thermopower is given by:

$$S(T) = \frac{2(\epsilon_f - \epsilon_F)T/e}{\left(\frac{3[(\epsilon_f-\epsilon_F)^2+\Gamma^2]}{(\pi k_B)^2}\right) + T^2} \qquad (2)$$

where ϵ_f is the position of the f-electron band and Γ the width of the Lorentzian peak. In figure 4 we include the results of fits to this expression of data above 500 K. We obtained $\epsilon_f - \epsilon_F = 40.5$ meV, $\Gamma = 227$ meV for UCu_5, and $\epsilon_f - \epsilon_F = 43.0$ meV, $\Gamma = 182$ meV for UCu_4Ag for the fit parameters, of the same order of magnitude as those reported by Tran *et al* for U_2Rh_2In [45]. Once again, it is clear that substitution of Cu by Ag produces only quantitative effects on the electronic structure of UCu_5. On the other hand, the $S(T)$ curve observed for UCu_4Ni shows a very different behaviour, impossible to analyse in terms of the model previously described. Notice the very weak temperature dependence between 300 and 650 K, with a negative slope above the maximum at 400 K. This indicates that, contrary to Ag, Ni substitution produces drastic changes in the electronic structure of UCu_5. In the context of the different theories of NFL behaviour enumerated above, the radical change in electronic structure produced by Ni doping explains the fast decrease of the Nèel temperature as a result of the imbalance between the RKKY and Kondo interactions. For UCu_4Ni, T_N tends to zero (a compositionally induced quantum critical point), and our XANES results show that this happens in the presence of structural disorder. This is just the magnetic Griffiths phase scenario proposed by Castro Neto *et al* [6]: the magnetic clusters induced by disorder close to this QCP give rise to Griffiths-McCoy singularities and NFL behaviour. This interpretation is in agreement with the analysis of the high field magnetization and ac susceptibility of this system recently reported by Lopez de la Torre *et al* [46].

4. Summary and conclusions

We have presented a detailed *ab initio* computation of the Cu K-edge XANES spectra in the case of UCu_5, UCu_4Ag and UCu_4Ni compounds performed within the multiple-scattering framework. The experimental spectra are well reproduced by computations performed using large clusters, ~6 Å around a central photoabsorbing atom, and by using the Dirac-Hara exchange and correlation potential. The comparison of the experimental and theoretical spectra unambiguously indicates the existence of Ag/Cu and Ni/Cu site interchange in UCu_4Ag and UCu_4Ni compounds, respectively. From these results we conclude that the preferential substitution of Ag at the 4c positions, previously suggested [31], does not take place in UCu_4Ag. The existence of crystallographic disorder in both systems, as well as the results of thermopower measurements, which demonstrate the dramatic changes in the electronic structure produced by Ni doping, point to the imbalance between the RKKY and Kondo interactions as the source of the NFL behaviour observed in UCu_4Ni. In our opinion, our findings support an interpretation of the NFL behaviour in terms of the Griffiths phase model [46].

Acknowledgments

This work was partially supported by the Spanish CICYT (Grants MAT2005-06806-C04-04 and FIS2006-11022) and Junta de Comunidades de Castilla-La Mancha (Grant PAI-05-013). The synchrotron radiation experiments were performed at SPline (Proposal: 25-01-616). We are indebted to G R Castro for his help during the experimental work at SPline (ESRF). We wish also to acknowledge K A McEwen and M Ellerby for many friendly and fruitful discussions.

References

[1] Stewart G R 2001 *Rev. Mod. Phys.* **73** 797
[2] Seaman C L, Maple M B, Lee B W, Ghamaty S, Torikachvili M S, Kang J-S, Liu L Z, Allen J W and Cox D L 1991 *Phys. Rev. Lett.* **67** 2882
[3] Maple M B, Seaman C L, Gajewski D A, Dalichaouch Y, Barbetta V B, Andrade M C, Mook H A, Lukefahr H G, Bernal O O and MacLaughlin D E 1994 *J. Low Temp. Phys.* **95** 225
[4] von Löhneysen H 1999 *J. Magn. Magn. Mater.* **200** 532
[5] Bernal O O, MacLaughlin D E, Lukefahr H G and Andraka B 1995 *Phys. Rev. Lett.* **75** 2023
[6] Castro Neto A H and Jones B A 2000 *Phys. Rev.* B **62** 14975
[7] Miranda E and Dobrosavljevic V 2001 *Phys. Rev. Lett.* **86** 264
[8] Andraka B and Stewart G R 1993 *Phys. Rev.* B **47** 3208
[9] López de la Torre M A, Ellerby M, Watmough M and McEwen K A 1998 *J. Magn. Magn. Mater.* **177–181** 469
[10] For a review see for example Prins R and Koningsberger D (ed) 1988 *X-Ray Absorption: Principles, Applications, Techniques of EXAFS, SEXAFS, XANES* (New York: Wiley) and references therein
[11] Lee P A and Pendry J B 1975 *Phys. Rev.* B **11** 2795
[12] Natoli C R and Benfatto M, unpublished
Benfatto M, Natoli C R, Bianconi A, García J, Marcelli A, Fanfoni M and Davoli I 1986 *Phys. Rev.* B **34** 5774
[13] Ankudinov A L, Ravel B, Rehr J J and Conradson S D 1998 *Phys. Rev.* B **58** 7565
[14] Joly Y, Cabaret D, Renevier H and Natoli C R 1999 *Phys. Lett.* **82** 2398
[15] Joly Y 2001 *Phys. Rev.* B **63** 125120
[16] Hatada K, Hayakawa K, Benfatto M and Natoli C R 2007 *Phys. Rev.* B **76** 060102(R)
[17] Chaboy J, Maruyama H and Kawamura N 2007 *J. Phys.: Condens. Matter* **19** 216214
[18] Chaboy J, Nakajima N and Tezuka Y 2007 *J. Phys.: Condens. Matter* **19** 266206
[19] Hatada K and Chaboy J 2007 *Phys. Rev.* B **76** 104411
[20] McEwen K A, López de la Torre M A, Watmough M and Ellerby M 1997 *Physica* B **230–232** 59
[21] Watmough M, McEwen K A, Ellerby M and López de la Torre M A 1998 *J. Magn. Magn. Mater.* **177–181** 469
[22] Natoli C R, Benfatto M, Brouder C, Ruiz Lopez M F and Foulis D L 1990 *Phys. Rev.* B **42** 1944

[23] See for example Chaboy J and Quartieri S 1995 *Phys. Rev.* B **52** 6349 and references therein
[24] Natoli C R, Benfatto M, Della Longa S and Hatada K 2003 *J. Synchrotron Radiat.* **10** 26
[25] Mattheis L F 1964 *Phys. Rev.* A **133** 1399
Mattheis L F 1964 *Phys. Rev.* A **134** 970
[26] Norman J G 1974 *Mol. Phys.* **81** 1191
[27] Desclaux J P 1975 *Comput. Phys. Commun.* **9** 31
[28] Clementi E and Roetti C 1974 *At. Data Nucl. Data Tables* **14** 177
[29] Lee P A and Beni G 1977 *Phys. Rev.* B **15** 2862
[30] Krause M O and Oliver J H 1979 *J. Phys. Chem. Ref. Data* **8** 329
[31] Umari A M, Yakhmi J V, Nambudripad N, Iyer R M, Gupta L C and Vijayaraghaven R 1987 *J. Phys. F: Met. Phys.* **17** L25
[32] Chau R, Maple M B and Robinson R A 1998 *Phys. Rev.* B **58** 139
[33] Booth C H, MacLaughlin D E, Heffner R H, Chau R, Maple M B and Kwei G H 1998 *Phys. Rev. Lett.* **81** 3960
[34] Bauer E D, Booth C H, Kwei G H, Chau R and Maple M B 2002 *Phys. Rev.* B **65** 245114
[35] Baenziger N C, Rundle R E, Snow A I and Wilson A S 1950 *Acta Crystallogr.* **3** 34
[36] Mixson D J, Kim J S, Swick M, Jones T, Stewart G R, Scheidt E-W, Scherer W, Murphy T and Palm E C 2006 *Phys. Rev.* B **73** 125016
[37] Doniach S 1977 *Physica* B **91** 231
Doniach S 1993 *Valence Instabilities and Related Narrow-Band Phenomena* ed R D Parks (New York: Plenum) p 435
[38] Ott H R, Rudigier H, Felder E, Fisk Z and Batlogg B 1985 *Phys. Rev. Lett.* **55** 1595
[39] López de la Torre M A, González J A, Izquierdo A, Vieira S, Ellerby M and McEwen K A 2000 *J. Appl. Phys.* **87** 5126
[40] vanDaal H J, Buschow K H J, van Aken P B and van Maaren M H 1975 *Phys. Rev. Lett.* **34** 1457
[41] Mott N F and Jones H A 1936 *The Theory of the Properties of Metals and Alloys* (Oxford: Clarendon)
[42] Dugdale J S 1977 *The Electrical Properties of Metals and Alloys* (London: Arnold)
[43] Hirst L L 1977 *Phys. Rev.* B **15** 1
[44] Gottwick U, Gloos K, Horn S, Steglich F and Grewe N 1985 *J. Magn. Magn. Mater.* **47/48** 536
[45] Tran V H and Bauer E 2006 *J. Phys.: Condens. Matter* **18** 4677
[46] López de la Torre M A, Durá O J, Ellerby M, McEwen K A and Maple M B 2008 *J. Magn. Magn. Mater.* **320** e443